



Cite this: *RSC Adv.*, 2021, **11**, 22571

## Preparation and characterization of novel bionanocomposites based on garlic extract for preserving fresh Nile tilapia fish fillets

Ahmed. M. Youssef,<sup>ID \*a</sup> Hoda S. El-Sayed,<sup>b</sup> Islam EL-Nagar<sup>a</sup> and Samah M. El-Sayed<sup>\*b</sup>

In this paper we describe the preparation of a new bionanocomposite based on carboxymethyl cellulose (CMC), Arabic gum (AG) and gelatin (GL), incorporating garlic extract (GE) and  $TiO_2$  nanoparticles ( $TiO_2$ -NPs). The prepared bionanocomposites were evaluated using X-ray diffraction (XRD), Fourier-transform infrared spectroscopy (FTIR), Energy Dispersive X-ray Analysis (EDX), and scanning electron microscopy (SEM), and were evaluated for their antimicrobial effect. The permeability and thermal and mechanical properties of the films were assessed. The water vapor transmission rate (WVTR), oxygen transmission rate (OTR), and mechanical, thermal and antimicrobial properties of the prepared bionanocomposite films were enhanced by the addition of GE and  $TiO_2$ -NPs. The effects of GE and  $TiO_2$ -NPs in combination incorporated into a CMC/AG/GL blend as an edible coating on the quality of fresh Nile tilapia fish fillets during refrigerated storage were evaluated. The microbiological status and weight loss of fresh Nile tilapia fish fillets were periodically tested for 21 days during storage at 4 °C. The results indicated that GE combined with  $TiO_2$ -NPs has a synergistic influence on the enhancement of the preservation properties of CMC/AG/GL/GE- $TiO_2$  bionanocomposites for refrigerated tilapia fish fillets, which could control microbial growth, and decrease weight loss during the storage of tilapia fish fillets.

Received 16th May 2021

Accepted 19th June 2021

DOI: 10.1039/d1ra03819b

rsc.li/rsc-advances

### 1. Introduction

Nano-coating technology is an effective way in which to extend the shelf life of food products. This technology uses metal nanoparticles such as titanium dioxide, copper oxide, zinc oxide, and silver and gold nanoparticles, plus hydrophilic and lipophilic materials such as plant extracts or other carbohydrates to produce antimicrobial and antioxidant activity to enhance the shelf life of various products.<sup>1-3</sup> Active packaging is an effective way to eliminate spoilage in food products like cheese, fruits, meat, and fish, which rapidly spoil and become unsafe for consumption.<sup>4-9</sup>

Research into bionanocomposite materials for use in food packaging and food contact surfaces is expected to increase over the next decade, with the development of new polymeric materials and composites including inorganic nanoparticles.<sup>10</sup> Eco-friendly packaging materials are synthesized from macromolecules including polysaccharides and proteins. Many kinds of polysaccharides have been used in food packaging applications, including cellulose derivatives,<sup>11</sup> gums,<sup>12</sup> chitosan,<sup>13</sup> and

alginate.<sup>6</sup> Proteins such as gelatin have also been used for the preparation of biodegradable packaging.<sup>14</sup> Such biopolymers displayed have limitations in terms of material properties, including unsatisfactory mechanical strength, poor water vapor as well as oxygen barrier, and higher manufacturing cost, although they are good at forming films.<sup>15</sup>

Food spoilage and poisoning occurs when food becomes contaminated with pathogenic bacteria and other microorganisms. The usual approach to combating these pathogens is the use of antibiotics. However, the over-use of antibiotics can lead to the development of antibiotic resistance.<sup>16</sup> Therefore, natural antimicrobial agents from plant, animal, and microbial sources are often used as preservative agents.<sup>17,18</sup> Antimicrobials are added to food to eliminate natural spoilage and to control the growth of microorganisms, to improve food safety.<sup>19</sup> Adding antioxidants to food is becoming widely used as a method to extend the shelf life of different foods, and reduce nutritional losses by controlling oxidation.<sup>20-22</sup>

Garlic (*Allium sativum* L.) has been recognized for its medicinal properties in many cultures around the world. It is believed to have anti-cancer effects, to stimulate the immune function, reduce cardiovascular diseases, and to have antimicrobial and antioxidant effects.<sup>23</sup> Garlic is a member of the lily family (Liliaceae), and is widely used as a spice in food, and by traditional medicine practitioners in the treatment of bacteria related to issues such as dander, cough and rheumatism.<sup>24</sup>

<sup>a</sup>Packaging Materials Department, National Research Centre, 33 El Bohouth St. (former El Tahrir St.), Dokki, Giza, 12622, Egypt. E-mail: amyoussef27@yahoo.com; Fax: +20 33370931; Tel: +20 33322418

<sup>b</sup>Dairy Science Department, National Research Centre, 33 El Bohouth St. (former El Tahrir St.), Dokki, Giza, 12622, Egypt



Garlic extract has been shown to have widespread antibacterial activity, including effects on *Escherichia*, *Salmonella*, *Staphylococcus*, *Klebsiella*, *Proteus*, *Clostridium*, *Mycobacterium* and *Helicobacter* species.<sup>25–28</sup> Allicin is the main component of the antimicrobial activity of garlic. It is a volatile sulfur molecule with a distinct scent.<sup>28</sup> Allicin has also been found to act as an anti-fungal, anti-viral, and anti-parasitic agent,<sup>29</sup> the antioxidant activity of garlic has been attributed to sulfur-containing compounds.<sup>30</sup> Reiter *et al.*,<sup>31</sup> demonstrated that allicin displayed antimicrobial action against pathogenic bacteria in the lung. The antimicrobial activity of garlic extract is also produced by other hydrophobic compounds, such as vinyldithiins, ajoenes, and diallyl polysulfides.<sup>24,32</sup> Therefore, garlic extract can be used to reduce microbial contamination of food during storage. Garlic was shown to delay the rate of microbial spoilage and extend the shelf life of tuna fillets by six days during refrigerated storage.<sup>33</sup> Kombat *et al.*,<sup>34</sup> found that the use of garlic paste extended the shelf life of fresh Nile tilapia fish more than three days over that of a control.

We describe a procedure for the preparation of CMC/AG/GL/GE-TiO<sub>2</sub> bionanocomposites based on carboxymethyl cellulose (CMC), Arabic gum (AG), gelatin (GL) and titanium dioxide (TiO<sub>2</sub>-NPs) as well as different concentration of garlic extract (GE), using a solution casting technique. The physicochemical properties and antimicrobial activity of the resulting CMC/AG/GL/GE-TiO<sub>2</sub> bionanocomposites were investigated. These bionanocomposite materials are promising for use as antimicrobial agents. We tested their effects upon the preservation of fresh Nile tilapia fish fillets.

## 2. Materials and methods

### 2.1. Materials

Carboxy methyl cellulose (CMC), with a molecular weight  $4.2 \times 10^8$ , and a degree of substitution of 0.7 was purchased from Kelong Chemical Agent Factory, Chengdu, China. AG was provided by Alpha Chemica, Mumbai, India. Gelatin (GL) and titanium dioxide (P<sub>25</sub>, TiO<sub>2</sub>-NPs) with cross-sectional dimensions of about 21 nm were obtained from Sigma-Aldrich (St. Louis, MO). Extra-pure citric acid (CA) as a crosslinker was purchased from SDFCL Chem. Ltd. (Mumbai, India). Glycerol (99% purity) was supplied by Merck (Darmstadt, Germany) used as plastizer. Purple garlic bulbs were at six months of maturation were obtained from a farm in Giza Governorate, Egypt. The garlic was washed and then milled into small pieces with an electric mill, and stored in polyethylene bags until extraction. The solvent used was 99.5% ethanol and from ABCO CHEMIE, Gillingham England. Tilapia fish with average weight around 500 g for each one was obtained from Giza Governorate, Egypt. Distilled water was used in all preparation procedures.

**2.1.1. Pathogenic strains.** Pathogenic strains were collected from the Dairy Department at the National Research Centre, Egypt. They included *Bacillus cereus* B-3711; *Staphylococcus aureus* ATCC 6538; *Listeria monocytogenes* 598; *Escherichia coli* ATCC 8739; *Pseudomonas aeruginosa* ATCC 15442; *Salmonella typhimurium* 14028s; and *Candida albicans* ATCC 10231. The strains were incubated in nutrient broth at 35 °C for 24 h until

reaching a turbidity of 0.5, according to the McFarland standard.

### 2.2. Methods

**2.2.1. Preparation of solvent garlic extracts.** Twenty-five grams of freshly minced garlic bulbs was extracted three times with 400 ml ethanol at room temperature with stirring for 3 h. Each extract was filtered through Whatman no. 1 filter paper, and the solvent was evaporated to dryness using a rotary evaporator under reduced pressure at 40 °C.<sup>35</sup> The extract was then kept in the dark in sterile screw capped bottles and stored at –20 °C until needed.

**2.2.2. Fish filleted samples preparation.** Fresh tilapia (*Oreochromis niloticus*) was washed, cleaned, beheaded, and filleted with a sharp stainless steel knife, washed with cooled water again, and drained for twenty minutes on a sterile stainless steel slab, as illustrated by Etemadian *et al.*<sup>36</sup> The fish was then filleted and stored for later use.

**2.2.3. Preparation of CMC/AG/GL/GE-TiO<sub>2</sub> bionanocomposite.** The CMC/AG/GL/GE-TiO<sub>2</sub> bionanocomposites were prepared using a solution casting method according to Ahmadi *et al.*,<sup>37</sup> with some modifications. About 5.0% CMC solution was prepared through dissolving 25 g CMC in 500 ml distilled water, and prepared 5% AG and 5% gelatin using the same method. CMC/AG/GL blends were produced by mixing the three polymer solutions at a ratio of 40% : 40% : 20%. The bionanocomposites were prepared by gradually adding a 3% TiO<sub>2</sub>-NPs suspension solution to the CMC/AG/GL solution (1 mg ml<sup>–1</sup> in water) and sonicating for 2 h at 25 °C using a Q500 Sonicator at a sonication power of 500 W, a frequency of 20 kHz, and an amplitude of 50%. Then, 30% wt/wt of CA was added to the polymer blend with continuous mechanical stirring. After that, the mixture was cured at 140 °C for 15 minutes to cross-link the blend. The solution was left to cool at room temperature, and then 20% wt/wt glycerol was added. GE was added at proportions of (2%, 4%, and 8%). The homogeneous suspensions solutions of CMC/AG/GL/GE-TiO<sub>2</sub> bionanocomposite were transferred into Teflon Petri dishes and port at room temperature for 72 h in order to evaporate the solvent and allow a film to form.

**2.2.4. Coating fresh Nile tilapia fish fillets.** Previously prepared fish fillets were separated into six groups. The first one was a control group, without coating, the second and the third were coated with biocomposites films based on CMC/AG/GL (Blank1) and CMC/AG/GL/TiO<sub>2</sub>-NPs (Blank 2), neither of which included GE. The fourth, fifth, and sixth groups were coated with CMC/AG/GL/GE-TiO<sub>2</sub> bionanocomposite suspensions contain 2% GE-TiO<sub>2</sub>, 4% GE-TiO<sub>2</sub> and 8% GE-TiO<sub>2</sub> respectively. All groups were stored at 5 °C ± 1 °C for subsequent microbiological quality assessment, which was performed within 21 days, to determine the overall quality of fish.

**2.2.5. Detection of antimicrobial effects of CMC/AG/GL/GE-TiO<sub>2</sub> bionanocomposite films.** The antimicrobial activity of CMC/AG/GL, CMC/AG/GL/TiO<sub>2</sub>-NPs and different CMC/AG/GL/GE-TiO<sub>2</sub> bionanocomposite solutions was examined using



nutrient agar and the well diffusion agar method published by Youssef, *et al.*<sup>8</sup> For each strain, 0.1 ml of the bionanocomposite solutions was feast on the surface of a plate filled with nutrient agar media. The plates were left for 2 h to allow the pathogens to saturate the agar. Wells were prepared in the agar layer with a 0.5 cm cork borer. Each well was filled with 100  $\mu$ l of a bionanocomposite solution. The diameter of the clear inhibition zone surrounding the wells was measured after the plates were incubated for 24 h at 37 °C. The antimicrobial activity of GE was examined in the same manner.

### 2.3. Characterizations

**2.3.1. X-ray diffraction.** The crystallographic structure of TiO<sub>2</sub>-NPs, CMC/AG/GL blend, CMC/AG/GL/TiO<sub>2</sub> bionanocomposites as well as the CMC/AG/GL/GE-TiO<sub>2</sub> bionanocomposites containing different ratios of garlic extract, (2% and 8%) were tested using a Philips X-ray diffractometer (PW 1930 generator, PW 1820 goniometer, Netherlands) armed by Cu K $\alpha$  radiation (45 kV, 40 mA, and  $\lambda = 0.15418$  nm). Using a range of  $2\theta$  from 5 to 70° thru step size of 0.05 as well as a counting time per step was 2 s per step.

**2.3.2. Fourier transmission infrared spectroscopy (FT-IR).** FT-IR spectroscopy in transmission mode was used to recognize the functional groups of the GE, CMC/AG/GL blend, CMC/AG/GL/TiO<sub>2</sub> bionanocomposites along with the CMC/AG/GL/GE-TiO<sub>2</sub> bionanocomposites containing different ratios of garlic extract, (2% and 8%). The FT-IR spectra were acquired by using a FTIR was measured using Bruker vertex 80 (Germany) in the range 4000–400  $\text{cm}^{-1}$  with resolution 4  $\text{cm}^{-1}$

**2.3.3. Transmission electron microscopy (TEM).** The morphology of the TiO<sub>2</sub> nanoparticles will be detected *via* transmission electron microscopy (JEOL Co., JEM-2100, Tokyo, Japan), below high-tension electricity of 160 kV at room temperature.

**2.3.4. Scanning electron microscopy (SEM) and EDX determination.** The morphology of the prepared TiO<sub>2</sub>-NPs, CMC/AG/GL blend, CMC/AG/GL/TiO<sub>2</sub> bionanocomposites along with the CMC/AG/GL/GE-TiO<sub>2</sub> bionanocomposites containing different ratios of garlic extract, (2% and 8%) were distinguished using SEM (High-Resolution Quanta FEG 250-SEM, Czech Republic).

**2.3.5. Thermogravimetric investigation.** TG study for all the prepared samples was accomplished by a LABSYS evo TGA STA DTA/DSC by Setaram A trademark of KEP Technologies group, France. From 6–10 mg bionanocomposite was weighed in an aluminum pan and then it was heated from ambient temperature up to 700 °C under nitrogen gas and at a heating ramping of 10 °C min<sup>-1</sup>.

**2.3.6. Water vapor and oxygen permeability measurements.** The permeability such as oxygen gas as well as water vapor transmission rates (OTR and WVTR) for CMC/AG/GL blend, CMC/AG/GL/TiO<sub>2</sub> bionanocomposites along with the CMC/AG/GL/GE-TiO<sub>2</sub> bionanocomposites containing different ratios of garlic extract, (2% and 8%) were carried out through the oxygen transmission rate (OTR). It is computed *via* means of an N530 Gas Permeability Analyzer (China), as per the

standards followed by ASTM D1434-82 (reapproved 2015). Also, the GBI W303 (B) Water Vapor Permeability Analyzer (China) was used for the determination of the WVTR through the cup method, using precise conditions of temperature (38 °C) and humidity (4%) as stated by the subsequent standards (ASTM E96). The apparatus used smooth and uniform plastic films with thickness of 200  $\mu\text{m}$  for both (GTR and WVTR). The assessment test was repetitive three times and the average values were recorded.

**2.3.7. Mechanical properties.** The mechanical properties of CMC/AG/GL blend, CMC/AG/GL/TiO<sub>2</sub> bionanocomposites along with the CMC/AG/GL/GE-TiO<sub>2</sub> bionanocomposites containing different ratios of garlic extract, (2% and 8%) parameters for example tensile strength and, elongation at break were studied using a Zwick (Germany) tensile testing machine (Model Z010) equipped with a load cell of 1 kN and a crosshead speed of 200  $\text{mm min}^{-1}$ , in accordance with ASTM D 882–18.

**2.3.8. Determination of phenol compounds for GE by high performance liquid chromatography (HPLC).** High performance liquid chromatography investigation was done *via* an Agilent 1260 series. The separation process was done by Eclipse C18 column (4.6 mm  $\times$  250 mm i.d., 5  $\mu\text{m}$ ). The mobile phase containing (A) water and (B) trifluoroacetic acid in acetonitrile (0.05%) at a flow rate 1  $\text{ml min}^{-1}$ . It was set sequentially in a linear gradient as follows: 0 min (82% A); 0–5 min (80% A); 5–8 min (60% A); 8–12 min (60% A); 12–15 min (85% A) and 15–16 min (82% A). The multi-wavelength detector was monitored at 280 nm. The injection volume was 10  $\mu\text{l}$  for each of the sample solutions. The column temperature was maintained at 35 °C.

**2.3.9. Determination of antioxidant activity of the GE and CMC/AG/GL/GE-TiO<sub>2</sub> bionanocomposite films.** The antioxidant activity of the garlic extract and CMC/AG/GL/GE-TiO<sub>2</sub> bionanocomposite film samples was estimated using 2,2-diphenyl-1-picrylhydrazil (DPPH) radical scavenging, as published by Jongjareonrak *et al.*<sup>38</sup> The absorbance was measured at 517 nm and the inhibition of DPPH-radical scavenging activity was measured using the subsequent equation:

$$\text{DPPH inhibition\%} = ((A^c - A^s)/A^c) \times 100$$

where,  $A^s$  is the sample absorbance and  $A^c$  is the absorbance of the control sample.

**2.3.10. Determination of total phenolic content of GE as well as CMC/AG/GL/GE-TiO<sub>2</sub> bionanocomposites films.** The total phenolic content of the garlic extracts and the fabricated CMC/AG/GL/GE-TiO<sub>2</sub> bionanocomposite film samples was assessed colorimetrically using a Folin–Ciocalteau reagent as described by Lafka *et al.*<sup>39</sup> The total phenolic content was calculated using a standard curve constructed using gallic acid as a standard, and was measured as mg gallic acid equivalent (GAE g<sup>-1</sup>).

**2.3.11. Weight loss of coated fish fillets.** All fish fillets were individually weighted at the start of the experiment and during storage. The weight loss (WL) was calculated as follows:

$$\text{WL\%} = ((W_{\text{ini}} - W_t)/W_{\text{ini}}) \times 100$$



where  $W_{\text{ini}}$  is the initial weight and  $W_t$  is the weight at time  $t$ .

**2.3.12. Microbiological evaluation of coated fish fillets during cold storage.** Several dilutions of the fish samples were prepared. At each sampling interval, 10 g of fish fillets was mixed thoroughly with a sterile saline solution (0.85% NaCl) for 1 min to prepare the initial dilution ( $10^{-1}$ ). Serial dilutions were plated on plate count agar (Merck, Germany) for total aerobic bacterial counts (TABC), followed by incubation at 35 °C for 48 h.<sup>40</sup> Samples for total anaerobic bacterial counts (TANBC) were plated on plate count agar and anaerobically incubated 48 h at 35 °C.<sup>40</sup> Enterobacteriaceae counts were carried out using violet red bile glucose agar (oxide), with the plates incubated for 24 h at 37 °C.<sup>41</sup> *Staphylococci* counts were performed by spreading 0.1 ml of a suitable dilution on the surface of a Baird Parker agar plates complemented with egg yolk and potassium tellurite solution and incubating for 48 h at 35 °C.<sup>41</sup> Counts of mold and yeast were performed by spreading 0.1 ml of a suitable dilution on the surface of rose bengal chloramphenicol agar plates and aerobically incubated at 25 °C for four days.<sup>42</sup> Finally, psychotropic bacteria were detected using plate count agar and incubated at 5 °C for seven days.<sup>41</sup> All microbiological results were expressed as  $\log_{10}$  CFU g<sup>-1</sup>.

#### 2.4. Statistical analysis

Statistical analysis of the obtained results evaluations was performed using means of three replicates  $\pm$  S. E using software.<sup>43</sup> The results were expressed as mean  $\pm$  standard error and the differences between means were tested for significance using Duncan's multiple range tests at ( $p \leq 0.05$ ).

### 3. Results and discussion

#### 3.1. X-ray diffraction (XRD) examination of the prepared bionanocomposite films

XRD patterns are used to study the physical properties of crystalline structures, and evaluate the compatibility of all constituent material in composite films. Fig. 1a shows the XRD

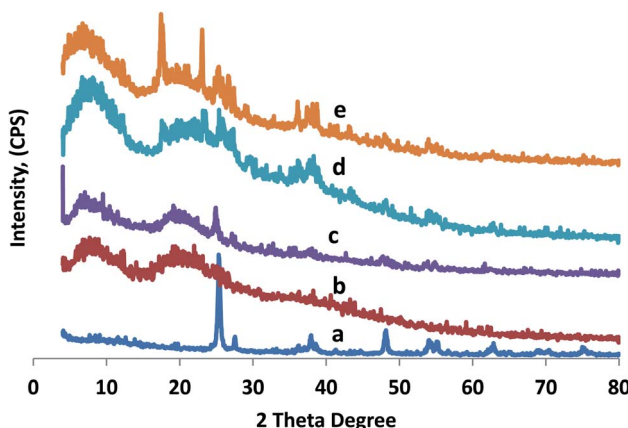


Fig. 1 XRD of (a) TiO<sub>2</sub>-NPs, (b) CMC/AG/GL blend, (c) CMC/AG/GL/TiO<sub>2</sub> bionanocomposites as well as the CMC/AG/GL/GE-TiO<sub>2</sub> bionanocomposites containing different ratios of garlic extract, (d) 2% and (e) 8%.

patterns of the fabricated TiO<sub>2</sub>-NPs. The majority of diffraction peaks matched the rutile phase of TiO<sub>2</sub>-NPs with some anatase phase. The diffraction peaks of 2 theta were observed at 27.30°, 35.36°, 37.67°, 39.86°, 41.4°, 56.76°, 61.85°, 73.32°, and 77.09°, which match the rutile phase of TiO<sub>2</sub>-NPs.<sup>44</sup> Additional crystal phases concerning to peaks at 25.17°, 47.84°, 53.68°, 56.02°, 68.38°, and 70.07° correspond to the anatase phase.<sup>45</sup> Fig. 1(b-e) shows the diffractogram patterns at 2 theta, which are identical at 6.40° and 20° for the CMC/AG/GL blend, CMC/AG/GL/TiO<sub>2</sub> bionanocomposites and CMC/AG/GL/GE-TiO<sub>2</sub> bionanocomposites containing different ratios of garlic extract: 2% and 8%. This peak reflects the distance among amino acid remains alongside the helix, which is around 0.44 nm.<sup>46</sup> These diffractogram patterns matched all of the prepared bionanocomposites, and had peaks caused by the presence of TiO<sub>2</sub>-NPs in bionanocomposite film formulations with different loadings of GE. The CMC/AG/GL blend produced smaller peaks at about  $2\theta = 10^\circ$  for the prepared films. Generally, the detected peak area patterns gotten via XRD were analogous for all fabricated films, since there was no significant influence of the GE on the polymer crystallinity, as shown in (Fig. 1d and e).

#### 3.2. FT-IR examination

Fourier transform infrared spectroscopic (FT-IR) investigation provides information about the functional properties of functional groups, as well as the structure of blended CMC/AG/GL composite, and CMC/AG/GL/GE-TiO<sub>2</sub> bionanocomposite films. Fig. 2 shows the FT-IR spectra for garlic extract (GE), CMC/AG/GL blend, and CMC/AG/GL/TiO<sub>2</sub> bionanocomposites as well as CMC/AG/GL/GE-TiO<sub>2</sub> bionanocomposites containing different proportions of garlic extract. Fig. 2a, shows FT-IR spectrum of GE, including functional groups such as hydroxyl, carbonyl, and carboxylic. The broad band at

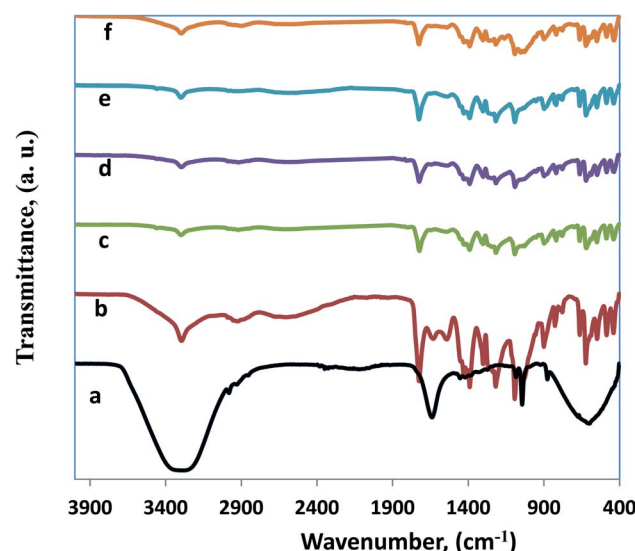


Fig. 2 FT-IR spectra for (a) garlic extract, (b) CMC/AG/GL blend, (c) CMC/AG/GL/TiO<sub>2</sub> bionanocomposites as well as the CMC/AG/GL/GE-TiO<sub>2</sub> bionanocomposites containing different ratios of garlic extract, (d) 2%, (e) 4%, and (f) 8%.



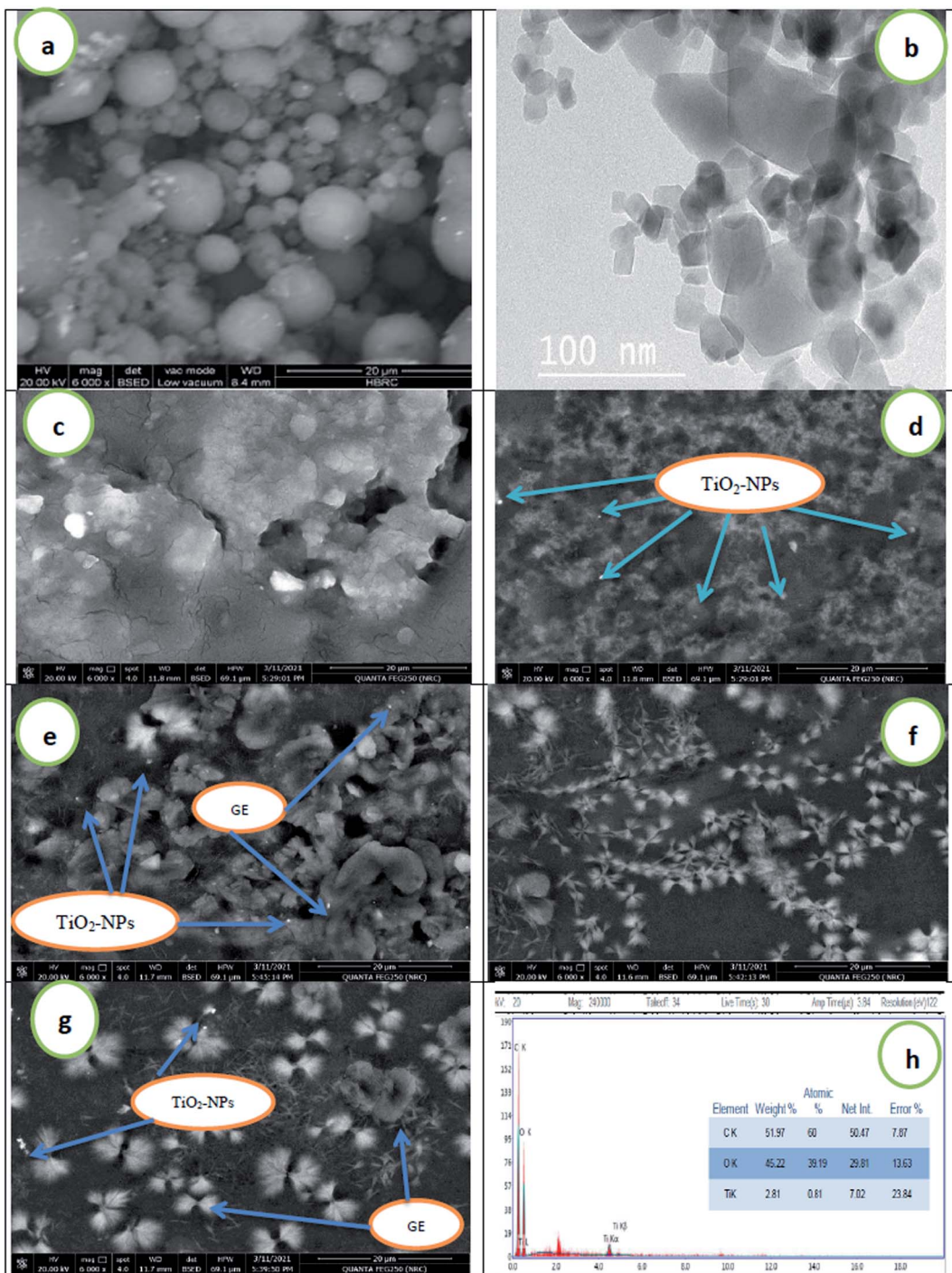


Fig. 3 (a) SEM of  $\text{TiO}_2$ -NPs, (b) TEM of  $\text{TiO}_2$ -NPs, (c) CMC/AG/GL blend, (d) CMC/AG/GL/ $\text{TiO}_2$  bionanocomposites, as well as CMC/AG/GL/GE- $\text{TiO}_2$  bionanocomposites containing different ratios from garlic extract, (e) 2%, (f) 4%, (g) 8% and, (h) EDEX analysis of CMC/AG/GL/ $\text{TiO}_2$  bionanocomposites containing 4% garlic extract.

$3370\text{ cm}^{-1}$  corresponds to the presence of O-H stretching of a hydroxyl group, showing the existence of polyhydroxy compounds such as saponins, flavonoids, and non-flavonoids. The band at  $2980\text{ cm}^{-1}$  is attributable to the asymmetric stretching of the C-H groups of aromatic compounds. The band at  $1660\text{ cm}^{-1}$  is due to C=O stretching of peptide connections and C=O stretching of carboxylic and carbonyl groups. The band at  $1380\text{ cm}^{-1}$  reflects the O-H bend of carboxylic acids

that in turn expose the attendance of tannins, saponins, glycosides, and flavonoids.<sup>35</sup> Also, Rastogi *et al.*,<sup>47</sup> recognized that the presence of peak for O-H group of carboxylic acids at  $1395\text{ cm}^{-1}$  that in turn displayed the existence of tannins, flavonoids, saponins as well as glycosides which matches with our results. Furthermore, the peak of S=O group at  $1036\text{ cm}^{-1}$  revealed the occurrence of organosulfur compounds comprising allicin, alliin, as well as diallyl disulphide.<sup>48</sup>

Fig. 2b, shows the FT-IR spectrum of the CMC/AG/GL blend. The FT-IR can recognize the effects of molecular interactions between CMC, AG, and gelatin, on the structure of a film. In Fig. 2b, the FT-IR spectra show the output of a CMC/AG/GL blend, which demonstrates different functional groups according to differences in drying conditions. Fig. 2b displays the CMC established film spectra with the adding of AG and gelatin, including bands of O-H stretching which shift near lower wavelengths ( $3328\text{ cm}^{-1}$ ). These shifts indicate that hydrogen bonds on OH groups in this blend were weaker than those in blank polymer films.<sup>49</sup> The amide II bands appear at  $1560\text{ cm}^{-1}$  for gelatin films. Bands at  $1689$ ,  $1616$  and  $1506\text{ cm}^{-1}$  designate C=O stretching (amide I) and NH bending (amide II) in the CMC/AG/GL blended films. Peaks at  $2989\text{ cm}^{-1}$  are produced by C-H stretching, and the films also showed peaks at about  $1420\text{ cm}^{-1}$  that arose from anti-symmetric as well symmetric COO- group vibrations. Therefore, mixing CMC with gelatin and AG produced a reduced intensity of the COO- group peak in our investigation, as presented in Fig. 2b.

Fig. 2c shows the FT-IR spectrum of CMC/AG/GL/TiO<sub>2</sub> bionanocomposites containing 1% TiO<sub>2</sub>-NPs. A band at  $3326\text{ cm}^{-1}$  corresponds to the stretching vibration of the hydroxyl group of the TiO<sub>2</sub>-NPs. The band near  $1610\text{ cm}^{-1}$  is attributable to Ti-OH; and a noticeable band at  $1371\text{ cm}^{-1}$  is associated with Ti-O.<sup>50</sup> In the FT-IR spectra of CMC/AG/GL/GE-TiO<sub>2</sub> bionanocomposites containing different ratios of garlic extract (2% and 8%) all bands for garlic extract and TiO<sub>2</sub>-NPs appeared at the same wavenumbers in CMC/AG/GL/GE-TiO<sub>2</sub> bionanocomposites, as shown in (Fig. 2d and e).

### 3.3. Morphological studies

Fig. 3 shows scanning electron microscope (SEM) images of the surface morphology of TiO<sub>2</sub>-NPs, CMC/AG/GL blend, and CMC/AG/GL/TiO<sub>2</sub> bionanocomposites containing 1% TiO<sub>2</sub>-NPs, as well as CMC/AG/GL/GE-TiO<sub>2</sub> bionanocomposites containing different proportions of garlic extract, (2%, 4%, and 8%) based on polymer matrix concentration. From the SEM result it can be seen that TiO<sub>2</sub>-NPs are spherical in shape, with particle sizes around  $10\text{ }\mu\text{m}$ , as shown in Fig. 3a. The images of the CMC/AG/GL composite blend show a homogeneous surface with an absence of TiO<sub>2</sub>-NPs, as well as the compatibility between three biopolymers (Fig. 3c); while the addition of 1% TiO<sub>2</sub>-NPs to the CMC/AG/GL matrix produces a heterogeneous surface for CMC/AG/GL/TiO<sub>2</sub> bionanocomposites in the presence of TiO<sub>2</sub> nanoparticles, as revealed in Fig. 3d. This is a result of the accumulation of TiO<sub>2</sub>-NPs throughout the film fabrication. The SEM images showed that spherical TiO<sub>2</sub>-NPs arise on the CMC/AG/GL bionanocomposite surfaces with an approximately uniform distribution. The bright zones indicate the crystalline TiO<sub>2</sub>-NPs, whereas the gray areas show the mostly amorphous CMC/AG/GL matrix, attributable to the high electron density of the TiO<sub>2</sub> nanoparticles.<sup>51</sup> An interface among TiO<sub>2</sub>-NPs and CMC/AG/GL was detected, which would result in enhanced properties of the fabricated CMC/AG/GL/TiO<sub>2</sub> bionanocomposites.

The addition of GE to the bionanocomposite matrix makes the surface more heterogeneous, due to the presence of the GE, which

appears as a flower structure in the bionanocomposite film (Fig. 3e-g). To further characterize the morphology of the TiO<sub>2</sub>-NPs, TEM analysis was performed. The TiO<sub>2</sub> nanoparticles were regular in shape, and occurred at the nanometer level, an observation which is in agreement with the XRD and SEM results. Fig. 3h shows the EDEX analysis of the CMC/AG/GL/GE-TiO<sub>2</sub> bionanocomposites, confirming the presence of TiO<sub>2</sub>-NPs in the polymer matrix.<sup>52</sup>

### 3.4. Thermal gravimetric analysis (TGA)

Fig. 4 shows the thermal stability of the prepared CMC/AG/GL blend, CMC/AG/GL/TiO<sub>2</sub> bionanocomposites, and CMC/AG/GL/GE-TiO<sub>2</sub> bionanocomposites containing different loadings of garlic extract (2%, 4% and, 8%). The proximate weight loses (%) and maximum temperature of degradation ( $T_{\text{max}}$ ) were determined from TGA curves. Three steps of WL (S1, S2 and S3, respectively) were detected for the CMC/AG/GL blend. In CMC/AG/GL/TiO<sub>2</sub> bionanocomposites the second step was overlapped with third, and just two steps were noted for CMC/AG/GL/GE-TiO<sub>2</sub> bionanocomposites containing different loadings of garlic extract (2%, 4%, and 8%). The S1 occurred at  $45\text{--}120\text{ }^{\circ}\text{C}$ , the S2 at  $115\text{--}235\text{ }^{\circ}\text{C}$  and S3 at  $235\text{--}450\text{ }^{\circ}\text{C}$ . The S1 is attributed to free water evaporation; S2 is attributed to loss of organic ingredients of CMC/AG/GL/GE-TiO<sub>2</sub> bionanocomposites and free glycerol evaporation, and S3 is ascribed to biopolymer branch degradation, as well as the rest of the glycerol and garlic extract volatile components. S1s of 5.4%, 5.2%, 4.6%, 4.4%, and 4.2% were assessed for CMC/AG/GL blend, CMC/AG/GL/TiO<sub>2</sub> bionanocomposites and for CMC/AG/GL/GE-TiO<sub>2</sub> bionanocomposites containing different loadings of garlic extract (2, 4 and, 8%), respectively. The  $T_{\text{max1}}$  for CMC/AG/GL blend was  $70.9\text{ }^{\circ}\text{C}$ , which was changed to  $74.5\text{ }^{\circ}\text{C}$  by the addition of TiO<sub>2</sub>-NPs for CMC/AG/GL/TiO<sub>2</sub> bionanocomposites. The addition of GE also improved the  $T_{\text{max1}}$  to  $76.2\text{ }^{\circ}\text{C}$ ,  $80.7\text{ }^{\circ}\text{C}$  and  $85.4\text{ }^{\circ}\text{C}$  for CMC/AG/GL/GE-TiO<sub>2</sub> bionanocomposites containing different loadings of garlic extract (2, 4 and, 8%), respectively.<sup>53</sup>

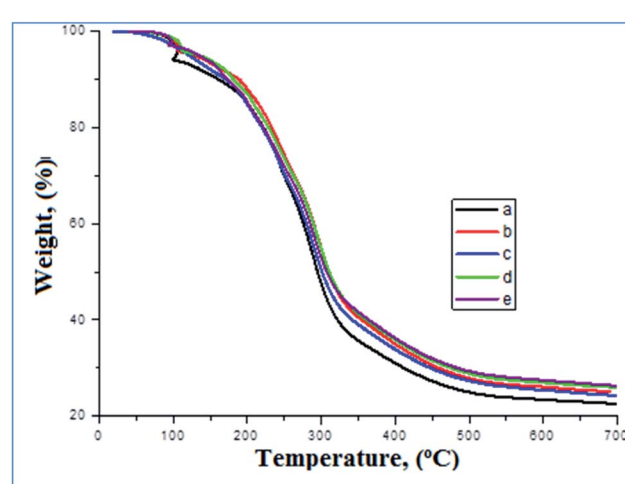


Fig. 4 TGA of (a) CMC/AG/GL blend, (b) CMC/AG/GL/TiO<sub>2</sub> bionanocomposites, as well as CMC/AG/GL/GE-TiO<sub>2</sub> bionanocomposites containing different ratios from garlic extract, (c) 2%, (d) 4%, and (e) 8%.



The S2 and S3 of 20.8% and 42.6% for CMC/AG/GL blend were reduced to 18.6% and 41.8% for CMC/AG/GL/TiO<sub>2</sub> bionanocomposites. The  $T_{\max 2}$  and  $T_{\max 3}$  were improved from 210.2 °C and 264.48 °C for the CMC/AG/GL blend to 215.4 °C and 266 °C for the CMC/AG/GL/TiO<sub>2</sub> bionanocomposites, respectively. An S2 of 60.8%, 61.2% and 61.6% and  $T_{\max 2}$  of 245.5 °C, 267.8 °C and 273.6 °C was determined for CMC/AG/GL/GE-TiO<sub>2</sub> bionanocomposites containing different loadings of garlic extract (2, 4 and, 8%), respectively. Associated with the CMC/AG/GL blend, the O-H interaction between biopolymers and TiO<sub>2</sub>-NPs, and the contamination of water and glycerol by adding TiO<sub>2</sub>-NPs and garlic extract is the most likely reason for higher  $T_{\max 1}$  &  $2$  in for CMC/AG/GL/TiO<sub>2</sub> bionanocomposites. The TiO<sub>2</sub>-NPs and GE therefore improved the evaporation temperatures of entrapped water and glycerol. The weight loses at higher temperatures (up to 500 °C) presented no certain peak, indicating that there is no discrete or main phase in bionanocomposite constituents with a definite TGA behavior. Also, the minor weight loses from 325 °C to 500 °C belongs to the residual fraction of volatile composites of GE and non-degraded CMC/AG/GL side-branches. The rise in total solid mass and the higher degradation temperature of TiO<sub>2</sub>-NPs led to higher heat stability of CMC/AG/GL/TiO<sub>2</sub> bionanocomposites and CMC/AG/GL/GE-TiO<sub>2</sub> bionanocomposites.

### 3.5. Mechanical properties investigations

Mechanical performance and properties are the most significant factors for packaging materials. Mechanical properties are important in marketing and protection of food products from damage during storage and transportation. Table 1 displays the mechanical properties of the CMC/AG/GL, CMC/AG/GL/TiO<sub>2</sub>, and CMC/AG/GL/GE-TiO<sub>2</sub> bionanocomposites comprising various ratios of garlic extract (2, 4, and 8%). The addition of TiO<sub>2</sub>-NPs produced important improvement in tensile strength (TS). While likened to the CMC/AG/GL blend, the TS increased from 38.70 MPa to 60.36 MPa by the adding of 1% of TiO<sub>2</sub> nanoparticles into the CMC/AG/GL matrix, while in the CMC/AG/GL/GE-TiO<sub>2</sub> bionanocomposites comprising diverse ratios of garlic extract (2, 4, and 8%) the TS values were increased to 65.76, 81.69 and 88.21 MPa with increases in the ratios (2, 4, and 8%) of garlic extract (GE) in the CMC/AG/GL blend. This rise in TS was accompanied by an initial rise in elongation at break for TiO<sub>2</sub>-NPs loading, and the elongation increased by increasing the loading of GE in CMC/AG/GL matrix, as shown in Table 1. This trend is normal, and attributed to the interaction between

the positive charges of TiO<sub>2</sub>-NPs and the negative charge of carboxylic groups of CMC/AG/GL blend in addition the change in the crystallinity, which are both important factors for the enhancement of tensile properties of the CMC/AG/GL/GE-TiO<sub>2</sub> bionanocomposites. The improvement in TS might also be related to the well dispersion of TiO<sub>2</sub>-NPs inside the polymer matrix that leads to a more uniform stress distribution, and reduces the occurrence of stress concentration centers.<sup>54</sup>

### 3.6. Permeability properties examinations

The permeability property of the prepared bionanocomposites is one of the most significant factors for the stability as well as shelf life of the foodstuff inside the bionanocomposites. The water vapor transmission rate (WVTR) and oxygen transmission rate (OTR) are dependent on various parameters, for example the type of polymer matrix, activation agent, additives, and the morphology of the prepared bionanocomposite film. Table 1 shows the WVTR and OTR results. Adding TiO<sub>2</sub>-NPs and GE to the CMC/AG/GL matrix led to a significant decrease in both WVTR and OTR. The presence of TiO<sub>2</sub>-NPs within the CMC/AG/GL matrix decreased the WVTR from 1236 to 1116 g m<sup>-2</sup> per day, and the OTR from 40.34 to 27.97 g m<sup>-2</sup> per day. Addition of GE into the CMC/AG/GL/TiO<sub>2</sub> bionanocomposites by different loading (2, 4, and 8%) reduced the WVTR by 1053, 986, and 956 g m<sup>-2</sup> per day, respectively. The OTR also declined from 31.43, 36.20, and 36.47 g m<sup>-2</sup> per day with increased GE concentration.

This improvement in the permeability properties of the prepared CMC/AG/GL/GE-TiO<sub>2</sub> bionanocomposites is produced by TiO<sub>2</sub>-NPs and GE inside the bionanocomposite structure as nanofiller, and obstructive the paths might form longer routs for the transfer of water vapor molecules and oxygen gas, and lower the WVTR and OTR.<sup>55</sup> The initial hydrophilic interactions between TiO<sub>2</sub>-NPs and the polymer matrix would reduce water permeation from the cross-paths of the bionanocomposites matrix. The permeability of bionanocomposite films was improved through the adding of GE, dependent on the hydrophilic or hydrophobic nature of the fabricated bionanocomposite and GE constituents. The principal purpose for the water barrier properties of extract comprising bionanocomposite films was the establishment of hydrogen bonds and hydrophobic interactions among bionanocomposite matrix as well as GE constituents such as (chlorogenic acid, gallic acid, rutin, vanillin, and catechin as major compounds and methyl gallate, syringic acid, naringenin, querectin, coffeeic acid, pyro catechol, and ferulic acid as minor compounds).

**Table 1** The mechanical and permeability results of the prepared CMC/AG/GL, CMC/AG/GL/TiO<sub>2</sub> as well as the CMC/AG/GL/GE-TiO<sub>2</sub> bionanocomposites containing different ratios of garlic extract

Samples	GE, %	TiO <sub>2</sub> -NPs, %	OTR (g m <sup>-2</sup> per day)	WVTR (g m <sup>-2</sup> per day)	T. S, MPa	Elongation, (%)
CMC/AG/GL	0.00	0.00	40.34	1236	38.70	45.48
CMC/AG/GL/TiO <sub>2</sub>	0.00	3.00	27.97	1116	60.36	49.45
CMC/AG/GL/GE-TiO <sub>2</sub>	2.00	3.00	31.43	1053	65.76	55.86
CMC/AG/GL/GE-TiO <sub>2</sub>	4.00	3.00	36.20	986	81.69	61.50
CMC/AG/GL/GE-TiO <sub>2</sub>	8.00	3.00	36.47	956	88.21	81.21



### 3.7. Antimicrobial activity of different bionanocomposites films

Table 2 shows the antimicrobial effects of designated CMC/AG/GL, CMC/AG/GL/TiO<sub>2</sub>, and CMC/AG/GL/GE-TiO<sub>2</sub> bionanocomposites containing different ratios of GE against some pathogenic strains. The GE had antimicrobial activity when examined against the Gram-positive bacteria *S. aureus* and *B. cereus* and the Gram-negative bacteria *L. monocytogenes*, *S. typhimurium*, *P. aeruginosa* and *E. coli*, and the yeast *C. albicans*. The zone of inhibition for GE ranged between 10 and 22 mm. The diameter of the zone of inhibition increased significantly when GE was incorporated into CMC/AG/GL/GE-TiO<sub>2</sub> bionanocomposite solutions. The CMC/AG/GL/GE-TiO<sub>2</sub> emulsion had inhibition activity ranged between 10 to 15 mm against tested strains and this inhibition occurred from the effect of TiO<sub>2</sub> nanoparticles. The antimicrobial mechanism of TiO<sub>2</sub> was associated to reactive oxygen species (ROS) with high oxidative potentials in the presence of O<sub>2</sub>. ROS are responsible for the damage by oxidation of many organic structures of microorganisms. TiO<sub>2</sub>-NPs have ability to loss of membrane integrity caused by oxidation of phospholipids due to ROS such hydroxyl radicals and hydrogen peroxide, which led to an increase in the membrane fluidity, leakage of cellular content, and eventually cell lysis.<sup>3,53</sup>

The inhibition zone was significantly increased by the addition of different concentrations of GE. In the case of CMC/AG/GL/2% GE-TiO<sub>2</sub> bionanocomposite solution, the zone of inhibition was recorded between 11 to 18 mm depending on the strain. But this inhibition was significantly enhanced with emulsion in the case of CMC/AG/GL/4% GE-TiO<sub>2</sub>, in which the zone of inhibition ranged between 15 and 21 mm, and increased with the concentration of 8% GE as a coating solution for CMC/AG/GL/8% GE-TiO<sub>2</sub> bionanocomposites solution, in which the inhibition zone was between 20 and 25 mm. We found that *E. coli* and *P. aeruginosa* were the most sustainable strains to the GE and different designated nanoparticles coating emulsions. Moreover, in case that using CMC/AG/GL coating emulsion was not detectable any inhibition zone around the well in the Petri dishes, where using this coating as a negative control for others coating emulsions, as well to detect the antimicrobial activity was due to garlic concentration and TiO<sub>2</sub>.

Our findings agree with those of<sup>27,28</sup> that indicate that garlic essential oil possesses antimicrobial activity in a dose-

dependent process, besides the magnitude of activity be determined by the microorganism.<sup>56</sup> The maximum activity was observed contrary to *S. aureus* and *E. coli*. The antimicrobial mechanism of GE was proposed to be because of its contented of various sulfides that are capable of damage microbial cells through reacting using the sulphydryl (SH) groups of cellular proteins to create mixed disulfides. In addition, allicin can inhibit the formation of bacterial biofilms.<sup>32,57</sup> Casella *et al.*,<sup>58</sup> established that garlic oil had antimicrobial activity against *S. aureus*, *P. aeruginosa* and *E. coli*, and that the allyl group was necessary for this activity. Also, Wolde *et al.*,<sup>27</sup> detected that the highest yield potential of garlic extract was obtained from water followed by ethanol, chloroform and petroleum ether respectively. *E. coli* were so susceptible than *S. aureus* to the extracts. Magryś *et al.*,<sup>59</sup> found that the *Allium sativum* extract inhibited the growth of a broad range of bacteria, including multidrug-resistant strains with bactericidal or bacteriostatic effect. Depending on the organism, the susceptibility to fresh garlic extract was comparable to the conventional antibiotic gentamycin.

### 3.8. Antioxidant activity and total phenolic content and of GE and CMC/AG/GL/GE-TiO<sub>2</sub> bionanocomposite films

The antioxidant bionanocomposite packaging films are an original design for improving the stability of oxidation sensitive food products. Table 3 illustrates the total phenolic content and antioxidant activity (%) by DPPH of the fabricated bionanocomposite films including different concentrations of GE, ranging from 2 to 8 wt%. Both bionanocomposite films based on CMC/AG/GL and CMC/AG/GL/TiO<sub>2</sub> free garlic extract had the lowest antioxidant activity and total phenolic content, as shown in (Table 3). With the addition of GE to the bionanocomposite packaging material, the DPPH scavenging ratio increased to 47.22, 48.97 and 50.93%. The total phenolic content increased to 29.58, 30.17, and 39.92 mg g<sup>-1</sup> for bionanocomposite films contain 2% GE-TiO<sub>2</sub>, 4% GE-TiO<sub>2</sub> and 8% GE-TiO<sub>2</sub>, respectively. The antioxidant activity and total phenolic compound of GE were 73.61% and 497.50 mg g<sup>-1</sup> extract, which could be due to the strong natural bioactive components of GE, such as allicin, ajoenes, 1,2-vinyldithiin, allixin, S-allyl-cysteine, and diallyl polysulfides; a wide range of antioxidant agents.<sup>24,32,60</sup>

Table 2 The antimicrobial activity of different bionanocomposites films<sup>a</sup>

Tested strains	GE	CMC/AG/GL	CMC/AG/GL/TiO <sub>2</sub>	CMC/AG/GL/2% GE-TiO <sub>2</sub>	CMC/AG/GL/4% GE-TiO <sub>2</sub>	CMC/AG/GL/8% GE-TiO <sub>2</sub>
Diameter of inhibition zone (mm)						
<i>B. cereus</i>	20 <sup>Ab</sup>	N.D	7 <sup>Dd</sup>	11 <sup>Cc</sup>	15 <sup>Bd</sup>	20 <sup>Ac</sup>
<i>S. aureus</i>	19 <sup>Ac</sup>	N.D	11 <sup>Dc</sup>	17 <sup>Cab</sup>	20 <sup>Bb</sup>	24 <sup>Ab</sup>
<i>L. monocytogenes</i>	18 <sup>Bc</sup>	N.D	10 <sup>Dc</sup>	15 <sup>Cb</sup>	20 <sup>Bb</sup>	23 <sup>Ab</sup>
<i>E. coli</i>	22 <sup>Ba</sup>	N.D	15 <sup>Da</sup>	19 <sup>Ca</sup>	22 <sup>Ba</sup>	26 <sup>Aa</sup>
<i>P. aeruginosa</i>	20 <sup>Bb</sup>	N.D	13 <sup>Db</sup>	18 <sup>Ca</sup>	21 <sup>Ba</sup>	25 <sup>Aa</sup>
<i>S. typhimurium</i>	17 <sup>Bc</sup>	N.D	12 <sup>Cb</sup>	14 <sup>Cb</sup>	18 <sup>Bc</sup>	21 <sup>Ac</sup>
<i>C. albicans</i>	21 <sup>Ab</sup>	N.D	10 <sup>Dc</sup>	13 <sup>Cb</sup>	18 <sup>Bc</sup>	22 <sup>Ac</sup>

<sup>a</sup> N.D: not detectable. Means with capital letter superscripts indicate insignificant difference between rows and means with small letter superscripts indicate insignificant difference between columns.



Table 3 Total phenolic content and antioxidant activity of GE and different bionanocomposites coating films<sup>a</sup>

Samples	GE-TiO <sub>2</sub> %	Antioxidant activity, %	Total phenol content, mg g <sup>-1</sup>
GE	0.0	73.61 ± 0.12 <sup>a</sup>	497.50 ± 4.12 <sup>a</sup>
B1	0.0	41.49 ± 0.29 <sup>e</sup>	26.38 ± 0.18 <sup>f</sup>
B2	0.0	41.70 ± 0.44 <sup>e</sup>	24.00 ± 0.23 <sup>e</sup>
CMC/AG/GL	2.0	47.22 ± 1.28 <sup>d</sup>	29.58 ± 0.33 <sup>d</sup>
CMC/AG/GL	4.0	48.97 ± 0.22 <sup>c</sup>	30.17 ± 0.29 <sup>c</sup>
CMC/AG/GL	8.0	50.93 ± 0.51 <sup>b</sup>	39.92 ± 0.12 <sup>b</sup>

<sup>a</sup> All parameters are represented as means ± standard error. Means in the same column with different superscript letters are significantly different at  $p \leq 0.05$ .

Table 4 Phenol compounds for garlic extract (μg g<sup>-1</sup> extract)

Peak	Phenol compounds	Retention time (min)	Peak area	Conc. (μg g <sup>-1</sup> )
1	Gallic acid	3.08	94.67	96.01
2	Chlorogenic acid	3.64	229.59	187.44
3	Catechin	4.30	8.91	10.09
4	Methyl gallate	4.98	21.62	2.89
5	Syringic acid	5.67	5.18	2.26
6	Pyro catechol	6.12	1.04	1.03
7	Rutin	6.94	11.91	14.74
8	Caffeic acid	5.44	4.14	1.56
9	Vanillin	8.73	64.99	14.07
10	Ferulic acid	9.49	3.02	1.09
11	Naringenin	9.91	5.63	2.95
12	Quercetin	11.99	3.99	2.57

### 3.9. Phenolic compounds determination of GE by HPLC

Phenolic compounds are an important group of plant phytochemicals which purpose as anti-bacterial, antioxidants, and extra biological activities in foodstuffs.<sup>61</sup> The phenol

components and their concentration in garlic extract (μg g<sup>-1</sup> extract) were revealed in (Table 4). There are twelve components were recognized in garlic extract. The main phenolic compounds were noted as chlorogenic acid, gallic acid, rutin, vanillin, and catechin as major compounds. There are a seven negligible compounds smaller than (10 μg g<sup>-1</sup> garlic extract) such as, methyl gallate, syringic acid, naringenin, quercetin, caffeic acid, pyro catechol, and ferulic acid. Our results obtained for garlic extract by HPLC were similar to those reported by Nuutila *et al.*,<sup>30,61</sup> Sultana and Anwar,<sup>62</sup> which did not found noticeable amounts of myricetin and kaempferol.

### 3.10. Weight loss of fish fillets

The weight of the fish fillets was assessed weekly and weight losses were calculated as a ratio from the initial fish fillet weight. The weight losses of coated fish from the different treatments were less than that of those coated without the addition of GE-TiO<sub>2</sub> nanoparticles in the coat matrix (Fig. 5). Fish coated with 8% GE-TiO<sub>2</sub> bionanocomposite had the minimum WL of 0.91% after 21 days of storage time. A significant connection was established between WL and storage

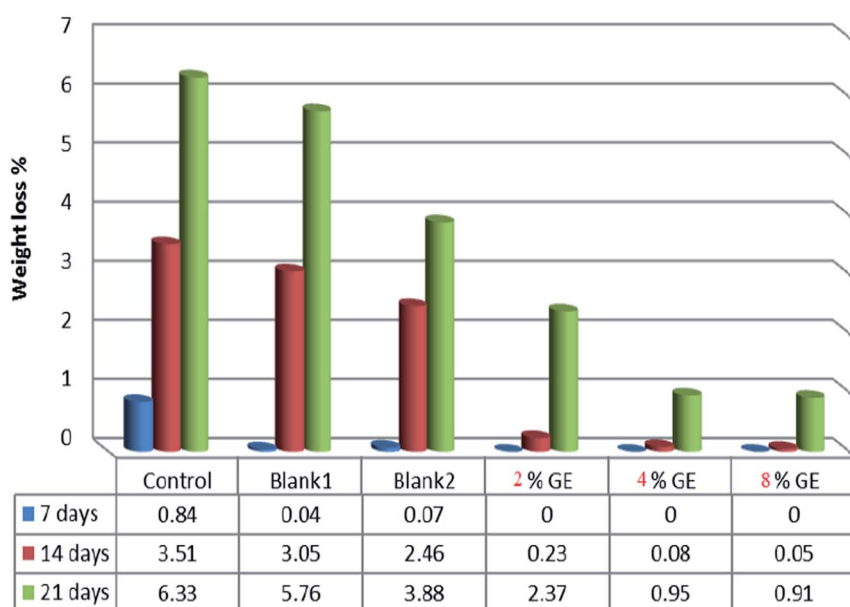


Fig. 5 Changes in weight loss values of control and coated fish fillets during storage as affected by coating.



period, and the observed behavior can be attributed principally to moisture loss. The low WL of fish fillets coated with GE-TiO<sub>2</sub> nanoparticles can be explained by the enhanced barrier properties the coating to water vapor. Similar findings were reported for cheeses coated with roselle extract (RE) combined with ZnO nanocomposites. El-Sayed *et al.*<sup>7</sup> found that an increasing ratio of roselle extract-ZnO nanocomposites in prepared bionanocomposites films decreased the extent of WVTR in these films.

### 3.11. Microbiological evaluation of coated fish fillets during storage

We recorded the microbiological changes to fish fillets during storage, to evaluate the effectiveness of different coated bionanocomposites for preservation of the samples. During storage, a gradually increase was witnessed in each sample, and significant variations were found among samples ( $P < 0.05$ ) as shown

in Fig. 6. The counts of Enterobacteriaceae in the first day of storage were  $2.07 \log_{10} \text{CFU g}^{-1}$  and after that, significant rises in all samples through storage were observed (Fig. 6A). At 21 days, the counts reached  $5.89, 4.90, 4.04, 3.69$  and  $3.00 \log \text{CFU g}^{-1}$  for coated fish fillets with CMC/AG/GL, CMC/AG/GL/TiO<sub>2</sub> bionanocomposites, as well as CMC/AG/GL/GE-TiO<sub>2</sub> bionanocomposites containing 2%, 4%, and 8% of garlic extract, respectively and the uncoated sample became contaminated at the same time. Fewer counts for Enterobacteriaceae were recorded for samples coated with CMC/AG/GL/GE-TiO<sub>2</sub> bionanocomposites containing 4% and 8% garlic extract.

The same trend in results was observed for total aerobic bacterial counts (TABC) (Fig. 6B). The TABC at the first day was  $3.60 \log_{10} \text{CFU g}^{-1}$  and it gradually increased during storage in all samples. The counts reached  $7.65, 6.59, 5.70, 5.25$  and  $5.10 \log_{10} \text{CFU g}^{-1}$  for coated fish fillets with CMC/AG/GL, CMC/

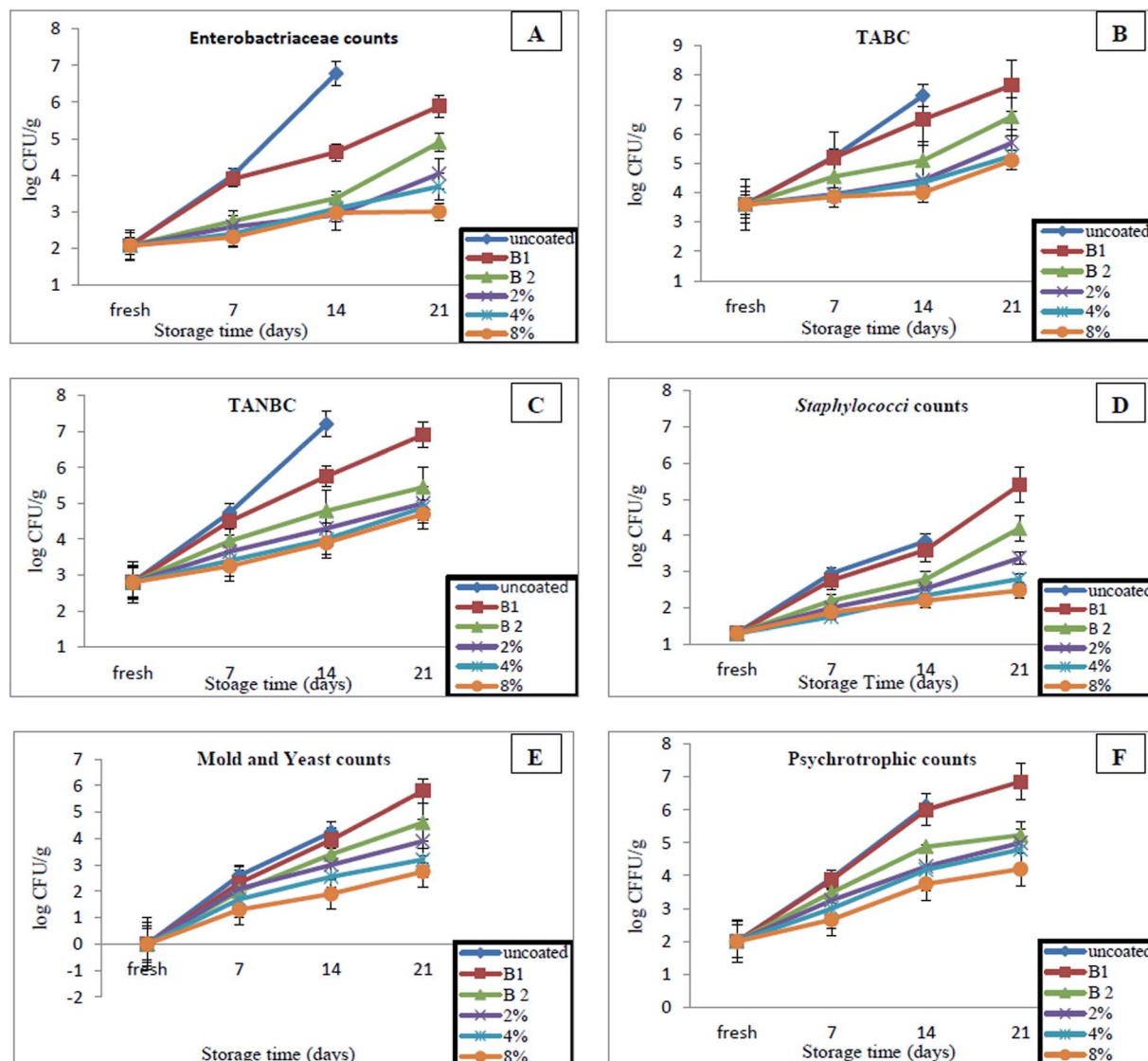


Fig. 6 Microbiological evaluation of coated fish fillets during cold storage. B1: CMC/AG/GL blend, B2: CMC/AG/GL/TiO<sub>2</sub> bionanocomposites, as well as CMC/AG/GL/GE-TiO<sub>2</sub> bionanocomposites containing different ratios from garlic extract, 2%, 4%, and 8%. All parameters are represented as means  $\pm$  standard error.



AG/GL/TiO<sub>2</sub> bionanocomposites, as well as CMC/AG/GL/GE-TiO<sub>2</sub> bionanocomposites containing 2%, 4%, and 8% of garlic extract, respectively at 21 days of storage. Also, not determined significant differences in the TABC between the coated samples with CMC/AG/GL/GE-TiO<sub>2</sub> bionanocomposites containing 2%, 4%, and 8% of garlic extract and the counts still fall within the acceptable levels  $6 \log_{10}$  CFU g<sup>-1</sup>.<sup>63</sup> Our results indicated TiO<sub>2</sub> with GE have anti-bacteriostatic activity, which was able to reduce the growth of bacteria compared with uncoated samples and samples coated with CMC/AG/GL film. Eisa *et al.*,<sup>64</sup> (2020) & Othman *et al.*,<sup>65</sup> showed that the TiO<sub>2</sub>-NPs exhibited potent antimicrobial activity against Gram-positive bacteria and Gram-negative bacteria.

The total anaerobic bacterial counts (TANBC) were recorded during cold storage (Fig. 6C). By first day, the TANBC were  $2.80 \log_{10}$  CFU g<sup>-1</sup>. The counts significantly increased over time during storage, but lower counts was recorded for the samples coated with CMC/AG/GL/GE-TiO<sub>2</sub> bionanocomposites containing 2%, 4%, and 8% of garlic extract than for samples coated with CMC/AG/GL film only. The uncoated samples become not save at 21 days, but the anaerobic counts were reached to 6.90 and 5.45 for coated samples with CMC/AG/GL and CMC/AG/GL/GE-TiO<sub>2</sub> bionanocomposites, respectively at the same time. The anaerobic counts in samples coated with CMC/AG/GL/GE-TiO<sub>2</sub> bionanocomposites containing 2%, 4%, and 8% garlic extract were around 1.90, 2.02 and 2.2 log cycles, compared with samples coated with CMC/AG/GL. Our data therefore confirmed the antimicrobial activity for GE with TiO<sub>2</sub>.

The safety of fish fillet samples were also assessed using counts of *Staphylococci* sp. during storage (Fig. 6D). When fresh, *Staphylococci* sp. was detected at around  $1.30 \log_{10}$  CFU g<sup>-1</sup>. The counts of *Staphylococci* sp. continuously increased with the time, and the most counts were detected for samples coated with CMC/AG/GL, followed by CMC/AG/GL/GE-TiO<sub>2</sub> bionanocomposites. Samples coated with CMC/AG/GL/GE-TiO<sub>2</sub> bionanocomposites containing 2%, 4%, and 8% of garlic extract had lower counts. These counts were recorded 3.38, 2.80 and  $2.48 \log_{10}$  CFU g<sup>-1</sup> for samples coated with CMC/AG/GL/GE-TiO<sub>2</sub> bionanocomposites containing 2%, 4%, and 8% of garlic extract, respectively at the end of storage. We did not observe significant differences in *Staphylococci* counts between samples coated with CMC/AG/GL/GE-TiO<sub>2</sub> bionanocomposites containing 4%, and 8% of garlic extract.

We also did not detect any mold or yeast in fresh samples (Fig. 6E). Small counts were detected at seven days of storage, and the counts gradually increased with storage. More counts were observed for samples coated with CMC/AG/GL ( $5.80 \log_{10}$  CFU g<sup>-1</sup>) followed by samples coated with CMC/AG/GL/GE-TiO<sub>2</sub> bionanocomposites ( $4.60 \log_{10}$  CFU g<sup>-1</sup>). The addition of GE enhanced the antimicrobial properties of coating bionanocomposites. The mold and yeast counts in samples coated with CMC/AG/GL/GE-TiO<sub>2</sub> bionanocomposites containing 2%, 4%, and 8% of garlic extract were lower by around 1.90, 2.60 and 3.05 log cycles, than samples coated with CMC/AG/GL only. The samples coated with CMC/AG/GL/GE-TiO<sub>2</sub> had counts about 1.2 less than samples coated with CMC/AG/GL, but uncoated samples became moldy by the end of storage.

The total psychrotrophic counts of samples were found to be near those of the uncoated samples during the first week of storage (Fig. 6F), however, after week, a slower increase in total psychrotrophic counts was observed for samples coated with CMC/AG/GL/GE-TiO<sub>2</sub> bionanocomposites containing 2%, 4%, and 8% of garlic extract compared with uncoated and CMC/AG/GL. Counts of 5.00, 4.80 and  $4.20 \log_{10}$  CFU g<sup>-1</sup> were obtained for the coated samples with CMC/AG/GL/GE-TiO<sub>2</sub> bionanocomposites containing 2%, 4%, and 8% of garlic extract, respectively, on the twenty-first day. The counts in samples coated with CMC/AG/GL and CMC/AG/GL/GE-TiO<sub>2</sub> bionanocomposites reached  $6.85$  and  $5.23 \log_{10}$  CFU g<sup>-1</sup>, respectively at the same time.

These microbiological results show that coating with bionanocomposites with TiO<sub>2</sub>-NPs plus GE was more effective in extending the shelf life of fish fillets for one week than uncoated samples and those coated with CMC/AG/GL only. These differences may be due to the GE antimicrobial activity,<sup>9,28,32,66</sup> plus the antimicrobial activity of TiO<sub>2</sub>-NPs.<sup>67</sup>

## 4. Conclusions

The current work showed that CMC/AG/GL/GE-TiO<sub>2</sub> bionanocomposites containing garlic extract had good thermal, mechanical and morphological properties. The Nile tilapia fish fillets coated with CMC/AG/GL/GE-TiO<sub>2</sub> bionanocomposites containing 4%, and 8% of GE successfully delayed bacteriological development, lost less water during cold storage for 21 days than uncoated samples, and had prolonged storage time one week than uncoated samples.

## Conflicts of interest

There are no conflicts to declare.

## References

- 1 H. Moustafa, S. M. El-Sayed and A. M. Youssef, Synergistic impact of cumin essential oil on enhancing of UV-blocking and antibacterial activity of biodegradable poly (butylene adipate-co-terephthalate)/clay platelets nanocomposites, *J. Thermoplast. Compos. Mater.*, 2021, DOI: 10.1177/0892705721989771.
- 2 A. M. Youssef and S. M. El-Sayed, Bionanocomposites materials for food packaging applications: Concepts and future outlook, *Carbohydr. Polym.*, 2018, **193**, 19–27.
- 3 A. M. Youssef, S. M. El-Sayed, H. S. El-Sayed, H. H. Salama, F. M. Assem and M. H. Abd El-Salam, Novel bionanocomposite materials used for packaging skimmed milk acid coagulated cheese (Karish), *Int. J. Biol. Macromol.*, 2018, **115**, 1002–1011.
- 4 B. W. Souza, M. A. Cerqueira, H. A. Ruiz, J. T. Martins, A. Casariego, J. A. Teixeira and A. A. Vicente, Effect of chitosan-based coatings on the shelf life of salmon (*Salmo salar*), *J. Agric. Food Chem.*, 2010, **58**(21), 11456–11462.
- 5 A. Abouel-Yazeed, Influence of Using Chitosan and Thyme during Cooling Storage of Sea Bass Fish, *Egypt. J. Food Sci.*, 2019, **47**(1), 115–130.



6 H. S. El-Sayed, S. M. El-Sayed, A. M. Mabrouk, G. A. Nawwar and A. M. Youssef, Development of eco-friendly probiotic edible coatings based on chitosan, alginate and carboxymethyl cellulose for improving the shelf life of UF soft cheese, *J. Polym. Environ.*, 2021, **29**(6), 1941–1953.

7 S. M. El-Sayed, H. S. El-Sayed, O. A. Ibrahim and A. M. Youssef, Rational design of chitosan/guar gum/zinc oxide bionanocomposites based on Roselle calyx extract for Ras cheese coating, *Carbohydr. Polym.*, 2020 Jul 1, **239**, 116234.

8 A. M. Youssef, F. M. Assem, H. S. El-Sayed, S. M. El-Sayed, M. Elaaser and M. H. Abd El-Salam, Synthesis and evaluation of eco-friendly carboxymethyl cellulose/polyvinyl alcohol/CuO bionanocomposites and their use in coating processed cheese, *RSC Adv.*, 2020, **10**(62), 37857–37870.

9 M. Rakshit and C. Ramalingam, Gum acacia coating with garlic and cinnamon as an alternate, natural preservative for meat and fish, *Afr. J. Biotechnol.*, 2013, **12**(4), 406–413.

10 A. Sorrentino, G. Gorrasi and V. Vittoria, Potential perspectives of bio-nanocomposites for food packaging applications, *Trends Food Sci. Technol.*, 2007, **18**(2), 84–95.

11 C. B. Francisco, M. G. Pellá, O. A. Silva, K. F. Raimundo, J. Caetano, G. A. Linde, N. B. Colauto and D. C. Dragunski, Shelf-life of guavas coated with biodegradable starch and cellulose-based films, *Int. J. Biol. Macromol.*, 2020, **152**, 272–279.

12 C. V. Dhumal, J. Ahmed, N. Bandara and P. Sarkar, Improvement of antimicrobial activity of sago starch/guar gum bi-phasic edible films by incorporating carvacrol and citral, *Food Packag. Shelf Life*, 2019, **21**, 100380.

13 N. A. Al-Tayyar, A. M. Youssef and R. R. Al-Hindi, Antimicrobial packaging efficiency of ZnO-SiO<sub>2</sub> nanocomposites infused into PVA/CS film for enhancing the shelf life of food products, *Food Packag. Shelf Life*, 2020, **25**, 100523.

14 L. Scartazzini, J. V. Tosati, D. H. Cortez, M. J. Rossi, S. H. Flôres, M. D. Hubinger, M. Di Luccio and A. R. Monteiro, Gelatin edible coatings with mint essential oil (*Mentha arvensis*): film characterization and antifungal properties, *J. Food Sci. Technol.*, 2019, **56**(9), 4045–4056.

15 L. Scartazzini, J. V. Tosati, D. H. Cortez, M. J. Rossi, S. H. Flôres, M. D. Hubinger, M. Di Luccio and A. R. Monteiro, Gelatin edible coatings with mint essential oil (*Mentha arvensis*): film characterization and antifungal properties, *J. Food Sci. Technol.*, 2019, **56**(9), 4045–4056.

16 P. K. Mukherjee, G. S. Saritha and B. Suresh, Antimicrobial potential of two different *Hypericum* species available in India, *Int. J. Phytother. Res.*, 2002, **16**(7), 692–695.

17 A. G. Ponce, S. I. Roura, C. E. del Valle and M. R. Moreira, Antimicrobial and antioxidant activities of edible coatings enriched with natural plant extracts: *in vitro* and *in vivo* studies, *Postharvest Biol. Technol.*, 2008, **49**(2), 294–300.

18 S. M. El-Sayed and H. S. El-Sayed, Antimicrobial nanoemulsion formulation based on thyme (*Thymus vulgaris*) essential oil for UF labneh preservation, *J. Mater. Res. Technol.*, 2021, **10**, 1029–1041.

19 M. E. El-Naggar, J. Hussein, S. M. El-sayed, A. M. Youssef, M. El Bana, Y. A. Latif and D. Medhat, Protective effect of the functional yogurt based on *Malva parviflora* leaves extract nanoemulsion on acetic acid-induced ulcerative colitis in rats, *J. Mater. Res. Technol.*, 2020, **9**(6), 14500–14508.

20 S. M. El-Sayed, Use of spinach powder as functional ingredient in the manufacture of UF-soft cheese, *Helijon*, 2020, **6**(1), e03278.

21 T. Tsuda, T. Osawa, K. Ohshima and S. Kawakishi, Antioxidative pigments isolated from the seeds of *Phaseolus vulgaris* L, *J. Agric. Food Chem.*, 1994, **42**(2), 248–251.

22 S. M. El-Sayed and H. S. El-Sayed, Production of UF-soft cheese using probiotic bacteria and *Aloe vera* pulp as a good source of nutrients, *Ann. Agric. Sci.*, 2020, **65**(1), 13–20.

23 I. GarbaI, A. I. Umar, A. B. Abdulrahman, M. B. Tijjani, M. S. Aliyu, U. U. Zango and A. Muhammad, Phytochemical and antibacterial properties of garlic extracts, *Bayero J. Pure Appl. Sci.*, 2013, **6**(2), 45–48.

24 G. El-Saber Batiha, A. Magdy Beshbishi, L. G. Wasef, Y. H. Elewa, A. A Al-Sagan, A. El-Hack, E. Mohamed, A. E. Taha, Y. M Abd-Elhakim and H. Prasad Devkota, Chemical constituents and pharmacological activities of garlic (*Allium sativum* L): A review, *Nutrients*, 2020, **12**(3), 872.

25 S. M. El-Sayed and A. M. Youssef, Potential application of herbs and spices and their effects in functional dairy products, *Helijon*, 2019, **5**(6), e01989.

26 A. Liaqat, T. Zahoor, M. Atif Randhawa and M. Shahid, Characterization and antimicrobial potential of bioactive components of sonicated extract from garlic (*Allium sativum*) against foodborne pathogens, *J. Food Process. Preserv.*, 2019, **43**(5), e13936.

27 T. Wolde, H. Kuma, K. Trueha and A. Yabeker, Anti-bacterial activity of garlic extract against human pathogenic bacteria, *J. Pharmacovigilance*, 2018, **6**(1), 1–5.

28 H. S. El-Sayed, R. Chizzola, A. A. Ramadan and A. E. Edris, Chemical composition and antimicrobial activity of garlic essential oils evaluated in organic solvent, emulsifying, and self-microemulsifying water based delivery systems, *Food Chem.*, 2017, **221**, 196–204.

29 M. A. Jabar and A. Al-Mossawi, Susceptibility of some multiple resistant bacteria to garlic extract, *Afr. J. Biotechnol.*, 2007, **6**(6), 771–776.

30 A. M. Nuutila, R. Puupponen-Pimiä, M. Aarni and K. M. Oksman-Caldentey, Comparison of antioxidant activities of onion and garlic extracts by inhibition of lipid peroxidation and radical scavenging activity, *Food Chem.*, 2003, **81**(4), 485–493.

31 J. Reiter, N. Levina, M. Van der Linden, M. Gruhlke, C. Martin and A. J. Slusarenko, Diallylthiosulfinate (Allicin), a volatile antimicrobial from garlic (*Allium sativum*), kills human lung pathogenic bacteria, including MDR strains, as a vapor, *Molecules*, 2017, **22**(10), 1711.



32 M. Nakamoto, K. Kunimura, J. I. Suzuki and Y. Kodera, Antimicrobial properties of hydrophobic compounds in garlic: Allicin, vinyldithiin, ajoene and diallyl polysulfides, *Exp. Ther. Med.*, 2020, **19**(2), 1550–1553.

33 K. K. Sathish, A. Jayakumari, K. Nagalakshmi and G. Venkateshwarlu, Shelf life extension of tuna fillets using natural preservatives isolated from garlic, *Fish. Technol.*, 2014, **51**, 179–186.

34 E. O. Kombat, M. S. Bonu-Ire, L. A. Adetunde and M. Owusu-Frimpong, Preservative effect of garlic (*Allium sativum*) paste on fresh Nile tilapia, *Oreochromis niloticus* (Cichlidae), *Ghana Journal of Science, Technology and Development*, 2017, **5**(1), 1–6.

35 K. Rajam, S. Rajendran and R. Saranya, *Allium sativum* (Garlic) extract as nontoxic corrosion inhibitor, *J. Chem.*, 2013, 2013.

36 Y. Etemadian, B. Shabanpour, A. S. Mahoonak and A. Shabani, Combination effect of phosphate and vacuum packaging on quality parameters of *Rutilus frisii* kutum fillets in ice, *Food Res. Int.*, 2012, **45**(1), 9–16.

37 R. Ahmadi, A. Tanomand, F. Kazeminava, F. S. Kamounah, A. Ayaseh, K. Ganbarov, M. Yousefi, A. Katourani, B. Yousefi and H. S. Kafil, Fabrication and characterization of a titanium dioxide ( $TiO_2$ ) nanoparticles reinforced bi-nanocomposite containing Miswak (*Salvadora persica* L.) extract—the antimicrobial, thermo-physical and barrier properties, *Int. J. Nanomed.*, 2019, **14**, 3439.

38 A. Jongjareonrak, S. Benjakul, W. Visessanguan and M. Tanaka, Effects of plasticizers on the properties of edible films from skin gelatin of bigeye snapper and brownstripe red snapper, *Eur. Food Res. Technol.*, 2006, **222**(3), 229–235.

39 T. I. Lafka, V. Sinanoglou and E. S. Lazos, On the extraction and antioxidant activity of phenolic compounds from winery wastes, *Food Chem.*, 2007, **104**(3), 1206–1214.

40 APHA, *Standard Methods for Examination of Dairy Products*, American Public Health Association, Washington, DC., USA, 16th edn, 1994.

41 FDA, Food and Drug Administration, *Bacteriological Analytical Manual*, AOAC International, Arlington, VA, USA, 9th edn, 2002, 56, pp. 4045–4056.

42 Rose Bengal Chloramphenicol (RBC) agar, *Culture Media for Food Microbiology*, ed. J. E. L. Corry *et al.*, 1995.

43 SAS, *Statistical Analyses systems, SAS, User Guide Statistics*, SAS Institute Inc., Cary, NC, 2004.

44 A. M. Youssef and F. M. Malhat, Selective removal of heavy metals from drinking water using titanium dioxide nanowire, *Macromol. Symp.*, 2014, **337**(1), 96–101.

45 H. Moustafa, A. M. Karmalawi and A. M. Youssef, Development of dapsoncapped  $TiO_2$  hybrid nanocomposites and their effects on the UV radiation, mechanical, thermal properties and antibacterial activity of PVA bionanocomposites, *Environ. Nanotechnol. Monit. Manag.*, 2021, **16**, 100482.

46 M. Alizadeh-Sani, A. Khezerlou and A. Ehsani, Fabrication and characterization of the bionanocomposite film based on whey protein biopolymer loaded with  $TiO_2$  nanoparticles, cellulose nanofibers and rosemary essential oil, *Ind. Crops Prod.*, 2018, **124**, 300–315.

47 L. Rastogi and J. Arunachalam, Sunlight based irradiation strategy for rapid green synthesis of highly stable silver nanoparticles using aqueous garlic (*Allium sativum*) extract and their antibacterial potential, *Mater. Chem. Phys.*, 2011, **129**(1–2), 558–563.

48 J. Songsungkan and S. Chanthai, Determination of synergic antioxidant activity of the methanol/ethanol extract of allicin in the presence of total phenolics obtained from the garlic capsule compared with fresh and baked garlic clove, *Int. Food Res. J.*, 2014, **21**(6), 2377.

49 Q. Tong and Q. Xiao, Preparation and properties of pullulan-alginate–carboxymethyl cellulose blend films, *Food Res. Int.*, 2008, **41**(10), 1007–1014.

50 S. Mugundan, B. Rajamannan, G. Viruthagiri, N. Shanmugam, R. Gobi and P. Praveen, Synthesis and characterization of undoped and cobalt-doped  $TiO_2$  nanoparticles via sol–gel technique, *Appl. Nanosci.*, 2015, **5**(4), 449–456.

51 P. Kaewklin, U. Siripatrawan, A. Suwanagul and Y. S. Lee, Active packaging from chitosan–titanium dioxide nanocomposite film for prolonging storage life of tomato fruit, *Int. J. Biol. Macromol.*, 2018, **112**, 523–529.

52 E. Farshchi, S. Pirsa, L. Roufegarinejad, M. Alizadeh and M. Rezazad, Photocatalytic/biodegradable film based on carboxymethyl cellulose, modified by gelatin and  $TiO_2$ –Ag nanoparticles, *Carbohydr. Polym.*, 2019, **216**, 189–196.

53 P. L. Barreto, A. T. Pires and V. Soldi, Thermal degradation of edible films based on milk proteins and gelatin in inert atmosphere, *Polym. Degrad. Stab.*, 2003, **79**(1), 147–152.

54 A. Vejdan, S. M. Ojagh, A. Adeli and M. Abdollahi, Effect of  $TiO_2$  nanoparticles on the physico-mechanical and ultraviolet light barrier properties of fish gelatin/agar bilayer film, *LWT–Food Sci. Technol.*, 2016, **71**, 88–95.

55 V. Bifani, C. Ramírez, M. Ihl, M. Rubilar, A. García and N. Zaritzky, Effects of murta (*Ugni molinae* Turcz) extract on gas and water vapor permeability of carboxymethylcellulose-based edible films, *LWT–Food Sci. Technol.*, 2007, **40**(8), 1473–1481.

56 V. P. Pavlović, J. D. Vujančević, P. Mašković, J. Ćirković, J. M. Papan, D. Kosanović, M. D. Dramićanin, P. B. Petrović, B. Vlahović and V. B. Pavlović, Structure and enhanced antimicrobial activity of mechanically activated nano  $TiO_2$ , *J. Am. Ceram. Soc.*, 2019, **102**(12), 7735–7745.

57 X. Y. Zhu and Y. R. Zeng, Garlic extract in prosthesis-related infections: a literature review, *J. Int. Med. Res.*, 2020, **48**(4), 1–10.

58 S. Casella, M. Leonardi, B. Melai, F. Fratini and L. Pistelli, The role of diallyl sulfides and dipropyl sulfides in the in vitro antimicrobial activity of the essential oil of garlic, *Allium sativum* L., and leek, *Allium porrum* L., *Phytother. Res.*, 2013, **27**(3), 380–383.

59 A. Magryś, A. Olander and D. Tchórzewska, Antibacterial properties of *Allium sativum* L. against the most emerging multidrug-resistant bacteria and its synergy with antibiotics, *Arch. Microbiol.*, 2021, 1–2.



60 A. Kopeć, E. Piatkowska, T. Leszczynska and E. Sikora, Healthy properties of garlic, *Curr. Nutr. Food Sci.*, 2013, **9**(1), 59–64.

61 M. E. Cartea, M. Francisco, P. Soengas and P. Velasco, Phenolic compounds in Brassica vegetables, *Molecules*, 2011, **16**(1), 251–280.

62 B. Sultana and F. Anwar, Flavonols (kaempferol, quercetin, myricetin) contents of selected fruits, vegetables and medicinal plants, *Food Chem.*, 2008, **108**(3), 879–884.

63 ICMSF, I., *Microorganisms in Foods, The International Commission on Microbiological Specifications for Foods of the International Union of Biological Societies*, 1986, pp. 181–196.

64 N. E. Eisa, S. Almansour, I. A. Alnaim, A. M. Ali, E. Algraby, K. M. Ortashi, M. A. Awad, P. Virk, A. A. Hendi and F. Z. Eissa, Eco-synthesis and characterization of titanium nanoparticles: Testing its cytotoxicity and antibacterial effects, *Green Process. Synth.*, 2020, **9**(1), 462–468.

65 S. H. Othman, N. R. Abd Salam, N. Zainal, R. Kadir Basha and R. A. Talib, Antimicrobial activity of  $\text{TiO}_2$  nanoparticle-coated film for potential food packaging applications, *Int. J. Photoenergy*, 2014, **2014**, 945930.

66 E. Aşik and K. Candoğan, Effects of chitosan coatings incorporated with garlic oil on quality characteristics of shrimp, *J. Food Qual.*, 2014, **37**(4), 237–246.

67 Y. Xing, X. Li, X. Guo, W. Li, J. Chen, Q. Liu, Q. Xu, Q. Wang, H. Yang, Y. Shui and X. Bi, Effects of Different  $\text{TiO}_2$  Nanoparticles Concentrations on the Physical and Antibacterial Activities of Chitosan-Based Coating Film, *Nanomaterials*, 2020, **10**(7), 1365.

